

## ON THE OPTICAL COUNTERPARTS, LONG-TERM VARIABILITIES, RADIO JETS, AND ACCRETION SOURCES IN 1E 1740.7–2942 AND GRS 1758–258

WAN CHEN<sup>1</sup> AND NEIL GEHRELS

NASA/Goddard Space Flight Center, Code 661, Greenbelt, MD 20771

AND

MARVIN LEVENTHAL

Department of Astronomy, University of Maryland, College Park, MD 20742

Received 1993 July 29; accepted 1993 November 11

### ABSTRACT

In this paper we discuss a variety of issues concerning the exciting and mysterious Galactic center  $\gamma$ -ray sources 1E 1740.7–2942 and GRS 1758–258. We discuss the problem associated with the highly uncertain X-ray absorption column toward 1E 1740.7–2942 and use the recent *ROSAT* results to narrow its range to  $0.5\text{--}1 \times 10^{23} \text{ cm}^{-2}$ . Then the current upper limits from deep optical and near-IR searches of stellar objects at these source locations are plotted on an H-R diagram, from which we find the mass of a potential companion star of the (supposed) black hole in GRS 1758–258 to be less than  $4 M_{\odot}$  and in 1E 1740.7–2942 to be less than  $9 M_{\odot}$ .

The observed well-collimated radio jets in 1E 1740.7–2942 require the existence of a stable accretion disk (presumably from binary accretion). The apparent association of 1E 1740.7–2942 with a high-density molecular cloud, on the other hand, points to possible accretion directly from the interstellar medium (ISM). We present an analysis of the energetics and kinematics of the radio jets in 1E 1740.7–2942. We find that the jets of 1E 1740.7–2942 are most probably made of normal proton-electron plasma (<20%) and electron-positron pairs. The observed good alignment of the radio core with its lobes implies that the source is moving in the ISM slowly ( $<10 \text{ km s}^{-1}$ ).

We present the long-term X-ray light curves of the two sources which include both the *Granat*/SIGMA's 3 yr monitoring data and all the data from previous imaging balloon and satellite observations over the last decade. The large amplitude, nonperiodic hard X-ray variabilities of these two sources appear to be similar, which suggest a common origin. The possible physical mechanisms responsible for producing *both* the long-term X-ray variations *and* the radio jets are postulated. Since the optical/near-IR and radio observations have excluded these systems as high-mass X-ray binaries like Cyg X-1 which accrete from strong stellar winds of massive companions, we consider Roche lobe-overflowing, low-mass X-ray binaries and Bondi-Hoyle accretion directly from a high-density surrounding medium. We propose a plausible scenario in which both sources are binary systems with a black hole primary and a low-mass companion and they are accreting mainly from the ISM at a rate self-regulated by the interaction between the accretion flow and the emerging hard X-ray flux.

*Subject headings:* black hole physics — Galaxy: center — gamma rays: observations —  
 ISM: jets and outflows

### 1. INTRODUCTION

#### 1.1. *The Excitement*

The Galactic center (GC) hard X-ray and low-energy  $\gamma$ -ray source 1E 1740.7–2942 has become one of the most exciting and mysterious sources in high-energy astrophysics. Discovered by the *Einstein*/IPC (Hertz & Grindlay 1984) as a weak soft X-ray (<4 keV) source located 50' from Sgr A\*, it was later found to be the dominant hard X-ray (>20 keV) source in the GC region (e.g., Skinner et al. 1991; Cook et al. 1991). Recently, the *Granat*/SIGMA coded-mask imaging telescope (35–1300 keV) revealed that 1E 1740.7–2942 is one of *only two* strong emitters above 100 keV within a few degrees of GC (the other one is GRS 1758–258, Sunyaev et al. 1991b), both are considered black hole candidates because they exhibit a Comptonized hard X-ray continuum similar to that of Cyg X-1 (Sunyaev et al. 1991a). A most remarkable (but short) outburst of broad positron annihilation radiation from 1E 1740.7–2942 was detected by SIGMA (Bouchet et al. 1991;

Sunyaev et al. 1991c), indicating it may contribute to the variable narrow 511 keV line radiation (Ramaty et al. 1992) observed from the GC direction by previous balloon and nonimaging satellite instruments (e.g., Lingenfelter & Ramaty 1989). The long-term continuum flux history of 1E 1740.7–2942 by SIGMA shows variability of amplitude greater than a factor of 5 on timescales of  $\sim 1$  yr and greater than  $\sim 20\%$  on day timescale (e.g., Cordier et al. 1993b).

The identification of 1E 1740.7–2942 in the radio has contributed significantly to our understanding. VLA observations (Prince & Skinner 1991) found two radio sources, A and B, in the IPC error box. Only source A appeared later in a smaller error box of a *Mir*/TTM hard X-ray image (Skinner et al. 1991), revealing it to be the counterpart. This identification was dramatically confirmed by the detection of a pair of well-collimated radio jets emanating from source A, i.e., the radio core which is now identified as the counterpart of 1E 1740.7–2942. Source B was found to be a radio lobe located at one end of the jets,  $\sim 30''$  (1 pc) from the core (Mirabel et al. 1992). Such a radio image closely resembles a microscale quasar, suggesting that 1E 1740.7–2942 is a stellar

<sup>1</sup> Universities Space Research Association.

mass black hole accreting from an accretion disk whose rotation axis and magnetic confinement define the jets (Mirabel 1992).

### 1.2. *The Mystery*

Binary accretion from a normal stellar companion is the most natural mechanism for the formation of the disk. The similarity between 1E 1740.7–2942 and Cyg X-1, which has an O9.7 Iab companion of  $25 M_{\odot}$  (e.g., Liang & Nolan 1984), also prompts one to look for a similar massive companion for 1E 1740.7–2942. Active searches in the optical and near-IR bands in the last few years, however, have not yet found any candidate (Prince & Skinner 1991; Skinner et al. 1991; Djorgovski et al. 1992; Leahy, Langill, & Kwok 1992; Mereghetti et al. 1992; Mirabel & Duc 1992). As we discuss below, this negative result may not be surprising if one considers the large absorption column toward 1E 1740.7–2942 derived from X-ray data (corresponding to  $\sim 30$  mag of visual extinction, Skinner et al. 1991; Sunyaev et al. 1991b). On the other hand, observations at millimeter wavelength revealed that 1E 1740.7–2942 lies on the line of sight to a dense ( $\sim 10^5 \text{ cm}^{-3}$ ) molecular cloud of  $10^5 M_{\odot}$  (Bally & Leventhal 1991; Mirabel et al. 1991), which may imply that (1) 1E 1740.7–2942 is deeply embedded in the cloud (which would be consistent with a large absorption column) so that the extremely high extinction prohibits us from detecting the companion star; or (2) there is no companion star and the source is simply accreting directly from the cloud.

Our understanding of 1E 1740.7–2942 may be enhanced by studying a similar GC  $\gamma$ -ray source, GRS 1758–258. The spectral shape, total luminosity, and long-term variability of the hard X-ray and low-energy  $\gamma$ -ray emission of GRS 1758–258 are remarkably similar to that of 1E 1740.7–2942 (Sunyaev et al. 1991b; Cordier et al. 1993b). Furthermore, recent deep VLA imaging has found that GRS 1758–258 also has radio jets and lobes (Rodriguez, Mirabel, & Marti 1992). It seems probable that these two  $\gamma$ -ray sources are the same class of objects and that progress on one source will help us to understand the other. The advantage for companion searches of GRS 1758–258 is that it has a smaller column depth (Sunyaev et al. 1991b; Skinner 1991), and there has been no evidence that it is associated with a molecular cloud. However, the most recent searches for its optical counterpart did not find any candidate either (Mereghetti et al. 1992; Leahy et al. 1992; Mirabel 1992).

In this paper we address the tantalizing question: *Why* has there been no optical counterpart found so far for either 1E 1740.7–2942 or GRS 1758–258? Is it because we have not looked hard enough? Or are the stars too dim or obscured to be detected? Or is there no stellar companion at all in these systems? The answer is closely related to a fundamental problem: *How* are the (supposed) black holes in these systems fed? By a companion star via a stellar wind or via Roche-lobe overflow? Or by the interstellar medium (ISM) via Bondi-Hoyle accretion? In § 2 we analyze the first question by discussing the current upper limits of the optical and near-IR counterpart searches (§ 2.1), the possible range of extinction toward these sources (§ 2.2), and then the constraints of these two quantities on the nature of the companions in an H-R diagram (§ 2.3). The important features in the long-term X-ray variations of these two sources are discussed in § 3. The radio jets and the implications to the source energetics and surrounding medium are discussed in § 4. Using the derived con-

straints on the companion star combined with those from the long-term X-ray and  $\gamma$ -ray variabilities and the radio jet-lobe structure, we consider various options and specific tests for and against the ISM (§ 5) and the binary accretion hypothesis (§ 6). A most promising scenario, low-mass binaries accreting from the ISM, is outlined in § 7. Finally, we summarize our results in § 8.

## 2. CONSTRAINT ON THE OPTICAL COUNTERPART

### 2.1. *The Current Upper Limits*

Early searches of the SERC *I* survey plates (Skinner et al. 1991) showed that no optical star down to  $I = 19$  appeared within  $10''$  of the VLA position of 1E 1740.7–2942 (source A). Subsequent observations in *I*, *K*, and *L* bands found no candidate within  $2''$  of the VLA position for either 1E 1740.7–2942 or GRS 1758–258 (Mereghetti et al. 1992; Leahy et al. 1992; Mirabel 1992; Djorgovski et al. 1992; Mirabel & Duc 1992), except in *L* a very marginal signal appeared close ( $\sim 1''$ ) to 1E 1740.7–2942 (Djorgovski et al. 1992). This signal is not seen in the *K* image which is 4 mag deeper than the *L* image. Because the VLA position of 1E 1740.7–2942 has sub-arcsecond accuracy, the weak *L* signal should still be regarded as an upper limit (Djorgovski et al. 1992). The current limiting optical and IR magnitudes for both 1E 1740.7–2942 and GRS 1758–258 are

$$I = 21, \quad K = 17, \quad L = 13 \quad (1)$$

(Mereghetti et al. 1992; Djorgovski et al. 1992; Mirabel 1992), except that the *L* limit applies to 1E 1740.7–2942 only.

### 2.2. *The Absorption Column Density*

The GC region exhibits high extinction due to the abundance of gas and dust. It is also populated with many dense, massive molecular clouds (Bally et al. 1988). However, outside the dense clouds, the extinction in the GC region follows a universal extinction law as in other directions (Savage & Mathis 1979; Rieke & Lebofsky 1985). The measurements of many bright late-type supergiants show that the GC extinction is between 23 and 36 mag in *V* (Lebofsky, Rieke, & Tokunaga 1982) which corresponds to an  $\text{H I}$  column density of between  $4.6 \times 10^{22} \text{ cm}^{-2}$  and  $7.2 \times 10^{22} \text{ cm}^{-2}$  (Savage & Mathis 1979).

There could be additional absorption if 1E 1740.7–2942 is physically associated with the nearby molecular cloud revealed by the millimeter observations. The cloud has an estimated total column density of  $2.8 \times 10^{23} \text{ cm}^{-2}$  from CO measurements (Bally & Leventhal 1991) and  $4.5 \times 10^{23} \text{ cm}^{-2}$  from  $\text{HCO}^+$  data (Mirabel et al. 1991). If 1E 1740.7–2942 is inside the cloud (assumed to be spherical) and its distance from the cloud core is the same as it is projected on the sky (cf. Fig. 6), an additional absorption column of 0.9 to  $1.4 \times 10^{23} \text{ cm}^{-2}$  from the cloud gives  $N_{\text{H}} \sim (1.4\text{--}2.1) \times 10^{23} \text{ cm}^{-2}$  toward 1E 1740.7–2942. Arguments concerning the scattered X-ray flux when the source was in the low state constrains its column density to be less than  $1.6 \times 10^{23} \text{ cm}^{-2}$  (Churazov et al. 1993a).

An accurate measurement of  $N_{\text{H}}$  toward 1E 1740.7–2942 from its soft X-ray spectrum would determine whether it is physically associated with the cloud. However, measurements by various space instruments, collected in Table 1, display large uncertainties and much model dependence. For ART-P-SIGMA data, the difference in  $N_{\text{H}}$  between different model

TABLE 1  
X-RAY SPECTRAL FITTING OF 1E 1740.7–2942<sup>a</sup>

Parameters	<i>Spartan 1</i> (0.7–15 keV)	TTM-HEXE (2–200 keV)	ART-P-SIGMA (3–1300 keV)
Observing epoch .....	1985 June	1989 March	1990 Apr
$L_{2-10 \text{ keV}}$ ( $10^{36} \text{ ergs s}^{-1}$ ) <sup>b</sup> .....	2.16	$2.79 \pm 0.29$	$6.8 \pm 0.4^c$
Bremsstrahlung $kT$ (keV) .....	$14.3^{+15.3}_{-5.4}$	$89^{+10}_{-9}$	$129 \pm 17$
$N_{\text{H}}$ ( $10^{23} \text{ cm}^{-2}$ ) .....	$1.45^{+0.26}_{-0.22}$	$2.58^{+1.30}_{-0.97}$	$0.4 \pm 0.7$
Reduced $\chi^2$ (dof) .....	0.66 (20)	1.45 (38)	0.85 (13)
Comptonization $kT$ (keV) .....	...	$18.8^{+1.5}_{-0.5}$	$41 \pm 2$
$N_{\text{H}}$ ( $10^{23} \text{ cm}^{-2}$ ) .....	...	$1.10^{+0.79}_{-0.50}$	$1.8 \pm 0.9$
Reduced $\chi^2$ (dof) .....	...	1.38 (37)	0.75 (11)
Power-law photon index .....	$2.00 \pm 0.35$	$1.0 \pm 0.1^d$	$1.84 \pm 0.04$
$N_{\text{H}}$ ( $10^{23} \text{ cm}^{-2}$ ) .....	$1.61^{+0.35}_{-0.29}$	$0.41^{+0.22}_{-0.20}$	$3.3 \pm 0.9$
Reduced $\chi^2$ (dof) .....	0.5 (26)	0.92 (37)	3.6 (12)

<sup>a</sup> Refs.: *Spartan 1* (Kawai et al. 1988); TTM-HEXE (Skinner et al. 1991); ART-P-SIGMA (Sunyaev et al. 1991a).

<sup>b</sup> Distance 8.5 kpc.

<sup>c</sup> (2–40 keV).

<sup>d</sup> Best fitting from a power law of the given photon index with exponential cutoff at 26.5 keV and  $e$ -folding energy of 52.8 keV.

fittings can be as high as a factor of 8, with the best-fit thermal bremsstrahlung model giving the lowest absorption column of  $0.4 \times 10^{23} \text{ cm}^{-2}$  to within a factor of 2. For the TTM-HEXE data, large discrepancies between different model fittings are also observed, and the best-fit power-law model with exponential cutoff also gives a low column density of  $0.4 \times 10^{23} \text{ cm}^{-2}$  with an uncertainty of 50%. *Spartan 1* was the most suitable instrument for measuring the absorption column and its results have the lowest statistical error ( $\leq 20\%$ ) and consistent values for the two model fittings (see Table 1). However, a rather high absorption column is obtained between 1.4 and  $1.6 \times 10^{23} \text{ cm}^{-2}$ .

The recent *ROSAT*/HRI (0.1–2 keV) observations of 1E 1740.7–2942 would have settled this dispute if the source had not plunged into a low state in 1991 with a flux drop, on average, of a factor of 5 below the normal state (Churazov et al. 1993a). However, as the *ROSAT* energy range is so sensitive to a high absorption column, even the weak detection of 1E 1740.7–2942 by the HRI in 1991 (Heindl et al. 1994) can still place a tight constraint on the column density. There is no good ART-P data available for the *ROSAT* observing date (1991 March 21). So, to determine this limit, we scale the normal state spectrum of 1E 1740.7–2942 down by a factor of 5 to calculate the expected HRI count rate and compare it with observations. The low energy ( $< 30 \text{ keV}$ ) part of the X-ray spectrum of 1E 1740.7–2942 in its normal state can be well fitted by an attenuated power law of photon index  $-1$  from the 1989 March TTM data (Skinner et al. 1991) and of photon index  $-1.8$  from the 1990 April ART-P data (Sunyaev et al. 1991b). The two spectra agree well at 20 keV with a flux of  $1.5 \times 10^{-3} \text{ photons s}^{-1} \text{ cm}^{-2} \text{ keV}^{-1}$  (i.e., TTM detected a flatter spectrum with lower luminosity, see Table 1). Since we do not know what kind of spectrum 1E 1740.7–2942 had when *ROSAT* observed it, we use two power-law slopes,  $-1$  and  $-2$ , to constrain the expected HRI total photon counts, in a 20 ks exposure, as a function of the absorption column. These two spectra are calibrated to the same flux at 20 keV which is taken to be a factor of 5 lower than the normal state. The results are plotted in Figure 1.

We see that the HRI response is very sensitive to column density. The weak detection ( $3 \sigma$ ) of 1E 1740.7–2942 restricts

the absorption column to a narrow range of between 5.3 and  $6.8 \times 10^{22} \text{ cm}^{-2}$  for the  $E^{-1}$  spectrum and between 0.95 and  $1.1 \times 10^{23} \text{ cm}^{-2}$  for the  $E^{-2}$  spectrum. The higher value is consistent with the lower bound of the *Spartan 1* results but definitely rules out a column density greater than  $1.6 \times 10^{23} \text{ cm}^{-2}$ . It is also clear that the major uncertainty in this analysis is from the unknown spectral shape during the observation. A simultaneous observation of *ROSAT* with *ASCA* would provide a precise measurement of the column density.

For GRS 1758–258, the ART-P spectrum gives only an upper limit of  $N_{\text{H}} < 7 \times 10^{22} \text{ cm}^{-2}$  (Sunyaev et al. 1991b). Searches in the *EXOSAT* and TTM databases (Skinner 1991) found that this source was detected by both instruments and the column density derived from the *EXOSAT*/ME spectrum (which has good low-energy coverage) is  $1.9 \times 10^{22} \text{ cm}^{-2}$ .

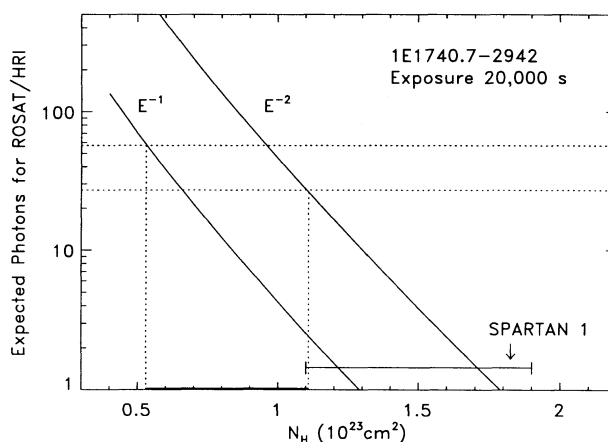


FIG. 1.—The total number of photons from 1E 1740.7–2942 in its low state expected to be detected by *ROSAT*/HRI during a 20,000 s observation, plotted as a function of the absorption column for two different continuum power-law models. The two models are calibrated to have the same flux at 20 keV and have photon spectral index of  $-1$  and  $-2$  as shown on the plot. The thick solid line on the bottom represents the uncertainty range of column density of the HRI results which are mostly due to the unknown spectral shape. For comparison, the range of the allowed column density from *Spartan 1* observations (Kawai et al. 1988) is also shown, which overlaps with the HRI results only at its lower energy range.

Thus, this source is *not* embedded inside a dense molecular cloud.

### 2.3. The Constraints on an H-R Diagram

From the observed optical and IR upper limits and the measured absorption column densities, we have calculated the limiting luminosity of the possible companion stars of 1E 1740.7–2942 and GRS 1758–258 as a function of the effective temperature and plotted the results on an H-R diagram (Fig. 2), using the formula

$$M_{\text{bol}} = X - A_X - DM + (V - X) + BC, \quad X = I, K, \text{ or } L, \quad (2)$$

where  $DM = 14.6$  is the distance modulus toward the GC,  $X$  is the observed optical or IR upper limit,  $A_X$  is the extinction in band  $X$ ,  $V - X$  is the IR color index, and  $BC$  is the bolometric correction. Both  $V - X$  and  $BC$  are functions of spectral type and luminosity class (Johnson 1966). For conversion between the column density and extinction for different bands, we use  $A_V = 5 \times 10^{-22} N_H$  (Savage & Mathis 1979), and  $A_I/A_V = 0.482$ ,  $A_K/A_V = 0.112$ , and  $A_L/A_V = 0.05$  (Rieke & Lebofsky 1985). In Figure 2, each of the  $I$ ,  $K$ , and  $L$  upper limits (eq. [1]) is represented by two curves of different extinction values.

We conclude from Figure 2 that an O9.7 Iab type companion, as for Cyg X-1, is ruled out for GRS 1758–258. In fact, the current  $K$  upper limit with an absorption column of  $1.9 \times 10^{22} \text{ cm}^{-2}$  ( $A_V = 9.5$ ) from *EXOSAT/ME* data (Skinner 1991) requires the companion star in GRS 1758–258 to be main sequence or subgiant less massive than  $\sim 4 M_\odot$ .

For 1E 1740.7–2942 an O star companion can also be ruled out, but *not* by the current IR upper limits on Figure 2 because of the large uncertainty in its column density. It is instead by

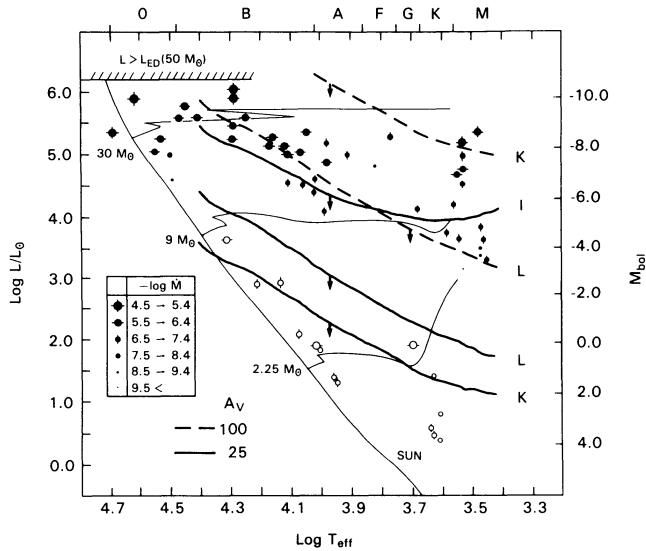


FIG. 2.—Current optical and near-IR upper limits on an H-R diagram. The limits are plotted according to two different values of the extinction as shown, which correspond to  $5 \times 10^{22} \text{ cm}^{-2}$  for  $A_V = 25$  and  $2 \times 10^{23} \text{ cm}^{-2}$  for  $A_V = 100$ . The  $I$ -band upper limit for  $A_V = 100$  is far off the scale of this plot and not shown. We see that for column density greater than  $1 \times 10^{23} \text{ cm}^{-2}$ , the  $L$ -band places more strict upper limits, otherwise the  $K$ -band data are more useful. For GRS 1758–258 with column density of  $2 \times 10^{22} \text{ cm}^{-2}$ , the upper limit on its companion mass (not shown) is clearly less than  $2 M_\odot$ . The original H-R diagram with stellar wind information (the filled and open circles) is from Cassinelli (1979).

the argument that the free-free radio flux from the compact H II region (created by the UV ionization radiation of an O star) would have been detected by VLA (Mirabel et al. 1991). In fact, the observed VLA  $\lambda 6 \text{ cm}$  flux from source A limits the companion star to be later than B2 (Mirabel et al. 1991), and the  $L$  upper limit curves in Figure 2 rule out a late-type supergiant ( $M_{\text{bol}} < -4$ ).

We see that for both 1E 1740.7–2942 and GRS 1758–258 a potential companion star can be neither an O star nor a red supergiant. More precisely, it can be no brighter than a giant star of  $9 M_\odot$  for 1E 1740.7–2942 and a subgiant of  $4 M_\odot$  for GRS 1758–258. We know that a companion star can power the compact object either by a Roche lobe overflow, as in cataclysmic variables and most low-mass X-ray binaries, or by a strong stellar wind as in Cyg X-1. So the question is, can we set any constraint on the binary parameters of these systems using the constraints on the stellar masses and luminosities we just learned? The answer is yes.

The mass-loss rates for stellar winds of various stars on the H-R diagram in Figure 2 (Cassinelli 1979) are represented by the sizes of the filled and open circles for normal stars and pre-main-sequence stars, respectively. It is clear that the wind mass-loss rate of a normal companion star for either 1E 1740.7–2942 or GRS 1758–258 must be less than  $10^{-8} M_\odot \text{ yr}^{-1}$ . (The pre-main-sequence stars, e.g., Herbig-Haro objects and T Tauri stars, usually have strong bipolar outflows as a result of the interaction between the star and its circumstellar disk [e.g., Shu, Adams, & Lizano 1987]. Since these young stars are unlikely to be the companions of  $\gamma$ -ray sources, their mass-loss rates are irrelevant to our discussions here).

On the other hand, the minimum wind mass-loss rate required to power the  $\gamma$ -ray sources can be derived by using the observed X-ray luminosity and the fact that, in a *detached* binary, the black hole can accrete no more than a few percent of the wind from a companion. The maximum fraction of the wind material which the black hole can accrete,  $\eta = \dot{M}_{\text{BH}}/\dot{M}_{\text{wind}}$ , scales roughly as the solid angle of its Roche surface as seen by the companion. This ratio depends largely only on the mass ratio of the system,  $q = m_{\text{BH}}/m_c$ , as

$$\eta = \frac{1}{2} \left( 1 - \cos \frac{RL_{\text{BH}}}{a} \right), \quad (3)$$

with

$$\frac{RL_{\text{BH}}}{a} = \frac{0.49q^{2/3}}{0.6q^{2/3} + \ln(1 + q^{1/3})},$$

(e.g., Livio 1994) where  $m_{\text{BH}}$  and  $m_c$  are the masses of the black hole and the companion,  $RL_{\text{BH}}$  is the Roche lobe radius of the black hole, and  $a$  is the binary separation. This result is illustrated in Figure 3. The peak X-ray luminosity of 1E 1740.7–2942 and GRS 1758–258 is  $\sim 10^{37} \text{ ergs s}^{-1}$  (e.g., Sunyaev et al. 1991b) which corresponds to a mass accretion rate of  $2 \times 10^{-9} M_\odot \text{ yr}^{-1}$  assuming a X-ray production efficiency of 0.1; it thus requires the companion star to have a wind stronger than  $10^{-7} M_\odot \text{ yr}^{-1}$  (the Cyg X-1 companion has a mass-loss rate of  $\sim 10^{-6} M_\odot \text{ yr}^{-1}$ ).

Therefore, it is clear that the potential companion star for either 1E 1740.7–2942 or GRS 1758–258 will *not* be able to feed the black hole via its stellar wind. If these  $\gamma$ -ray sources are powered by binary accretion, it can only be done via Roche lobe overflow; so they have to be *contact* binaries. By equating the stellar radius to its Roche lobe radius, we can determine the

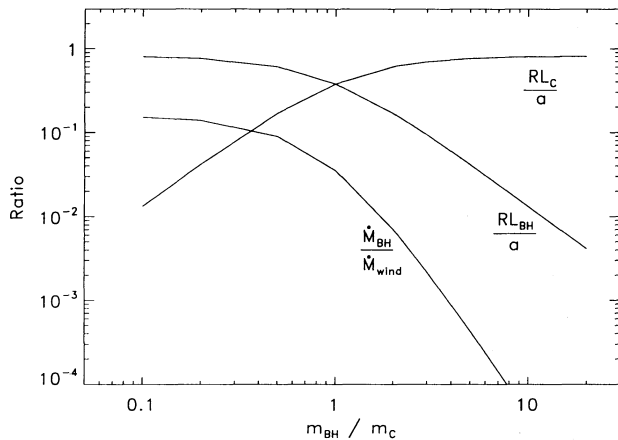


FIG. 3.—The maximum fraction of the companion stellar wind material which can be accreted by the black hole in a binary system,  $M_{\text{BH}}/M_{\text{wind}}$ , as a function of the mass ratio,  $m_{\text{BH}}/m_c$ , of the binary. Also shown are the ratio of each component's Roche lobe radius to the binary separation.

binary period of the system, as shown in Figure 4, if the masses of the black hole and the companion are known. From the above upper limits on the companion masses ( $< 4 M_{\odot}$ ) and the probable mass of the black holes ( $> 3 M_{\odot}$ ), the binary period in these systems is likely to be shorter than 20 hr.

### 3. THE LONG-TERM VARIABILITIES

One of the major discoveries after 3 yr of monitoring the GC by SIGMA is that 1E 1740.7–2942 and GRS 1758–258 are not only the brightest  $\gamma$ -ray sources in the region but also the most violent ones; their hard X-ray flux have shown large amplitude, long-term variabilities as well as day-to-day flickering (Cordier et al. 1993b; Gilfanov et al. 1993; Cordier, Paul, & Hameury 1993a; Mandrou et al. 1993). In 1990 when SIGMA started the monitoring program, the two sources were seen in a so-called normal state with an average flux (40–150 keV) of  $1.8 \times 10^{-2}$  photons  $\text{cm}^{-2} \text{s}^{-1}$  (120 mCrab) for 1E 1740.7–2942 (Cordier et al. 1993a) and  $1.3 \times 10^{-2}$  photons  $\text{cm}^{-2} \text{s}^{-1}$  (90 mCrab) for GRS 1758–258 (Gilfanov et

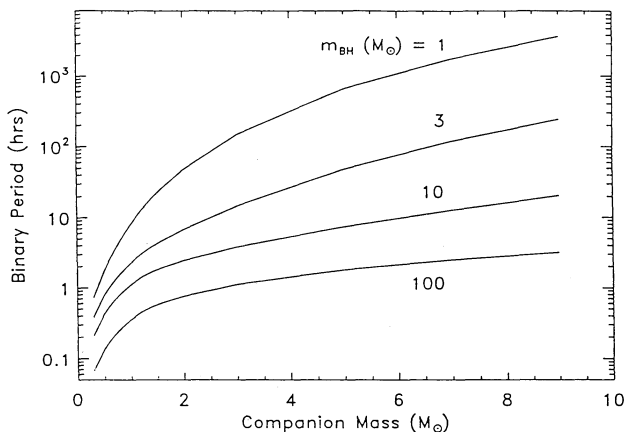


FIG. 4.—The expected binary period, if the black hole in a binary system is fed by Roche lobe overflow, as a function of the companion mass for four different black hole masses. For a nominal stellar black hole mass of a few ( $> 3$ ) solar masses, the binary period in 1E 1740.7–2942 and GRS 1758–258 is expected to be smaller than 20 hr.

al. 1993). The famous burst of broad annihilation radiation occurred in 1990 October. In the spring of 1991, 1E 1740.7–2942 plunged into a low state; its hard X-ray flux dropped by about a factor of 5. At the same time, GRS 1758–258's flux also started to decline, but only by about 30%. Both sources were seen in low states by the fall of 1991 and sometimes they fell below the detection limit of SIGMA (9 mCrab). In the spring of 1992, 1E 1740.7–2942 started to rise again, followed by GRS 1758–258 in the fall of 1992. Both sources were almost back to their normal states by the end of the year (Cordier et al. 1993b). From their previous behavior, one would have expected that these sources would be back to their normal states in 1993 and stay there for at least a few months. It is thus very surprising that the SIGMA observations in early 1993 found that both 1E 1740.7–2942 and GRS 1758–258 sank again into a low state followed by a steady recovery (Mandrou et al. 1993; E. Churazov, private communication).

In Figure 5, we have plotted the SIGMA light curves for 1E 1740.7–2942 and GRS 1758–258 and also a collection from the literature of all previous measurements from imaging balloon and satellite instruments. Most of the early observations (panel *a* and *b*) are at lower energies, so we used the simultaneous ART-P and SIGMA measurements in 1990 of the normal state of both sources as a calibration point. Notice that the low-energy fluxes of both sources in the Crab units are lower than those at high energies due to the flatter spectra than that of the Crab. There was no *Einstein*/IPC pointing near GRS 1758–258. There are several distinct features in these long-term X-ray light curves. (1) Except for the declining phase in the spring of 1991, the light curves of 1E 1740.7–2942 and GRS 1758–258 are quite similar; their hard X-ray fluxes vary on similar timescales and amplitudes. So the physical mechanisms producing the variabilities in these two systems may be similar. (2) The variations are nonperiodic (at least for 1E 1740.7–2942). From the SIGMA data alone, one might have the impression of a (quasi-) periodic trend. However, after including the data points from earlier observations, we see that the long-term variability of 1E 1740.7–2942 is not periodic. (3) During the last decade or so, 1E 1740.7–2942 seems to have stayed in the normal state longer than in the low state. Though the pre-SIGMA observations are sparse, it is unlikely that all the balloon and satellite observations (except *Einstein*/IPC) detected 1E 1740.7–2942 in the normal state just by chance. An detailed analysis of the data from the nonimaging balloon observations of the GC region in the last decade gives a similar assessment (Gehrels & Tueller 1993). For GRS 1758–258 such a trend is less obvious. (4) In the 30–150 keV range, the transitions between the normal and the low states of GRS 1758–258 are always smooth, but 1E 1740.7–2942 has never been caught during its transition from the normal state to the low state, as demonstrated by the three such transitions observed (Fig. 5c); the sharp flux declining between EXITE and POKER measurements in 1989 may indicate that such transitions in 1E 1740.7/2942 are always abrupt; the phase transition pattern is important to our understanding of the nature of the accretion in these systems. (5) The observed long-term variation timescale is limited by the observability of the GC region by *Granat*. It is possible that 1E 1740.7–2942 and GRS 1758–258 varied during the months SIGMA was not looking. On much shorter timescales, daily flux fluctuations of as much as 50% are observed superposed on the long-term variations.

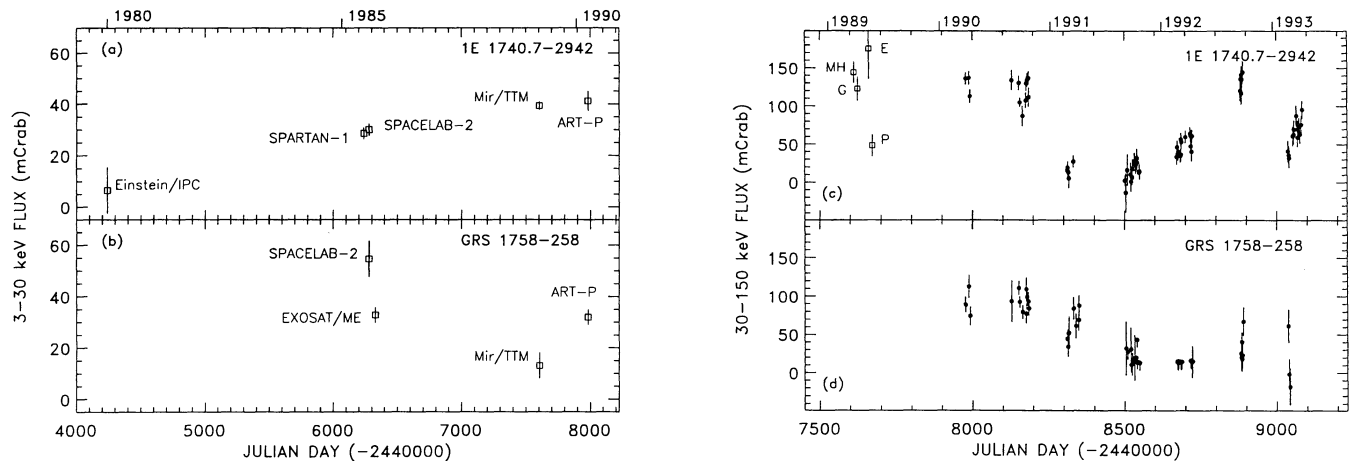


FIG. 5.—The long-term X-ray and  $\gamma$ -ray light curves of 1E 1740.7–2942 and GRS 1758–258 collected from all previous imaging balloon and satellite instruments. (a)–(b) The 3–30 keV light curves from 1980 to 1990. The data points are sparse. The *Einstein/IPC* (0.5–4 keV) and *Spartan 1* (0.5–10 keV) fluxes are calculated by extrapolating the observed soft X-ray flux to the 3–30 keV range for a power-law spectrum of  $E^{-2}$ . The large error bars in the IPC point are due to uncertainties in the column density and in early IPC response matrix (G. K. Skinner, private communication). (c) The 30–150 keV light curve of 1E 1740.7–2942 from 1989 to early 1993. The filled circles are SIGMA observations. Other earlier measurements as marked are *Mir/HEXE* (MH), GRIP (G), EXITE (E), and POKER (P). (d) The 30–150 keV SIGMA light curve of GRS 1758–258 in the same period. Notice that the normal state flux in 3–30 keV for both sources in Crab units is lower than that in 30–150 keV due to their flatter broad-band spectra than that of the Crab. The timescale in (a)–(b) is much longer than that in (c)–(d) but there is an 800 day overlap: the *Mir/HEXE* observations in (c) are simultaneous with *Mir/TTM* observations in (a)–(b).

REFS.—1E 1740.2942—*Einstein/IPC* (Hertz & Grindlay 1984); *Spartan 1* (Kawai et al. 1988); *Spacelab 2* (Skinner et al. 1987); *Mir/TTM-HEXE* (Skinner et al. 1991); POKER (Bazzano et al. 1992); GRIP (Cook et al. 1991); EXITE (Couvault, Manandhar, & Grindlay 1991); *Granat/ART-P-SIGMA* (Mandrou et al. 1993). GRS 1758–258—*Spacelab 2*, EXOSAT/ME and *Mir/TTM* (Skinner 1991); *Granat/ART-P-SIGMA* (Mandrou et al. 1993; Gilfanov et al. 1993).

The observed long-term hard X-ray variability is likely associated with the variations in the source energy supply, i.e., it reflects some (internal or external) systematic regulation processes of the mass accretion rate onto the compact object. So a change by a factor of 5 in the hard X-ray fluxes signals a similar change in their mass accretion rates. Although there are no soft X-ray light curves which would directly yield the variation of accretion rates through the accretion disks, this hypothesis gains strong observational support from the good correlation between the hard X-ray flux and the nonthermal radio flux observed from source A of 1E 1740.7–2942 (Mirabel et al. 1992).

#### 4. THE RADIO JETS

A most intriguing characteristic of 1E 1740.7–2942 and GRS 1758–258 is their radio jet-lobe structure (Mirabel et al. 1992; Rodriguez et al. 1992). Jets are commonly seen in active extragalactic nuclei and protostars in our own Galaxy (e.g., Burgarella, Livio, & O’Dea 1993), but they have not yet been found in X-ray binaries except, of course, in SS 433. Jets of normal gas may form when there is an accretion disk around a central object and part of the accretion flow through the disk is expelled from the central region by radiation pressure or other physical mechanisms. Electron-positron pair jets can form, for example, when pairs are produced via  $\gamma$ - $\gamma$  interactions in an intense radiation field in the deep potential well of a compact object and then driven out by the radiation pressure at near the speed of light. In reality a jet may be a mixture of normal plasma and  $e^+e^-$  pairs. The collimation of the jets is thought to be provided by the confining magnetic fields carried along with (or generated inside) the accretion flow (Begelman, Blandford, & Rees 1984). Thus the existence of a stable accretion disk is essential in forming, collimating, and sustaining the jets. The lobes, on the other hand, are the results of the interaction of the jets with a dense surrounding medium which may effectively

slow down the jets. Fast dissipation of the jet’s kinetic energy forms strong shocks which in turn (re) accelerate the energetic particles that cause enhanced local emissivity.

##### 4.1. Are the Jets Made of Pure Pairs?

We know that the jets from young stars are made of normal gas, but our knowledge of the composition of jets from black hole systems (e.g., AGNs) is very limited (e.g., Begelman et al. 1984) because of the lack of observational constraints. Whereas these jets are usually thought to be a mixture of the  $e^+e^-$  pairs and normal plasma, the question is, which component provides most of the momentum? Recent work (Cellotti & Fabian 1993) shows that jets in radio galaxies may be dominated by normal plasma, we shall try to answer this question for 1E 1740.7–2942 by estimating the maximum distance the jets can penetrate into the ISM.

There are two pieces of information here. One is the high gas pressure in the GC region (Blitz et al. 1993). In a molecular cloud (or the clumps inside a cloud) the gas density is in the range  $n_I \sim 10^4$ – $10^5$   $\text{cm}^{-3}$  and the temperature is 10–100 K, so the ISM pressure  $P_I/k = n_I T_I$  is of the order  $10^6$   $\text{cm}^{-3}$  K, where  $k$  is the Boltzmann constant, and  $n_I$  and  $T_I$  are the number density and temperature of the ISM. To be more precise, for the cloud projected near to 1E 1740.7–2942,  $n_I \approx 5 \times 10^4$   $\text{cm}^{-3}$  and  $T_I \approx 50$  K (e.g., Mirabel et al. 1992), which implies  $P_I/k \approx 2.5 \times 10^6$   $\text{cm}^{-3}$  K. This value should also apply to less dense (and so hotter) regions since the ISM phases are generally in pressure equilibrium.

The second piece of information is the maximum rate at which positrons are deposited into the ISM from 1E 1740.7–2942 via the jets. This can be inferred from the flux of the variable narrow 511 keV line observed from the GC region. Early observations give a relatively high value of  $\sim 10^{-3}$  photons  $\text{cm}^{-2}$   $\text{s}^{-1}$  (e.g., Ramaty & Lingenfelter 1991), but recent *GRO/OSSE* results have set an upper limit to the

flux from 1E 1740.7–2942 of  $3 \times 10^{-4}$  photons  $\text{cm}^{-2} \text{s}^{-1}$  (Purcell et al. 1992). SIGMA has imaged the GC region for more than 3 yr in the narrow 511 keV band and placed a  $3\sigma$  upper limit of  $2 \times 10^{-4}$  photons  $\text{cm}^{-2} \text{s}^{-1}$  for any persistent point sources of annihilation in the region (Roques 1993). This gives a maximum positron annihilation rate of  $2.6 \times 10^{42}$  positrons  $\text{s}^{-1}$  (assuming that about 90% of the annihilations are via positronium formation, Ramaty & Lingenfelter 1991). By considering the possibility that there may be other discrete positron sources in the GC region, we may conclude that the persistent positron production rate of 1E 1740.7–2942 is no greater than  $\sim 10^{42}$  positrons  $\text{s}^{-1}$ . One can also argue that 1E 1740.7–2942 produces positrons mostly in bursts as the one observed in 1990 October with an astonishing annihilation flux of  $1.2 \times 10^{-2}$  photons  $\text{s}^{-1}$  and lasted for about a day. However, since SIGMA has monitored the GC region for more than 1000 hr in the last 3 yr during which only 14 hr are recorded to show the strong annihilation feature, we may safely conclude that the duty cycle of large pair bursts is no more than 1%. This gives an averaged positron production rate of 1E 1740.7–2942 in bursts to be less than  $5 \times 10^{41}$  positrons  $\text{s}^{-1}$ . Here we assume that there is an equal number of pairs injected into the jets and annihilated near the black hole (e.g., Ramaty et al. 1992). Thus, the positron injection rate into the jets of 1E 1740.7–2942 from both the persistent and burst modes is likely to be  $\dot{N}_+ \leq$  a few  $\times 10^{42}$  positrons  $\text{s}^{-1}$ .

A jet will eventually be stopped at large distance when its ram pressure is balanced by the thermal pressure of the ISM gas,  $\rho_j v_j^2 = n_I k T_I$ , where  $\rho_j$  and  $v_j$  are the mass density and internal speed of the jet. The density of a mixed jet (if not much contaminated on its way by the ISM) can be estimated as a function of its opening angle  $\theta$  and the distance from the central source  $r$ , by considering that the mass injection rate into a single jet,  $\dot{M}_j \equiv m_e \dot{N}_+ + m_p \dot{N}_p/2 = \pi \theta^2 r^2 \rho_j v_j/4$ , i.e.,

$$\rho_j = \left(1 + \frac{f m_p}{2 m_e}\right) \frac{4 m_e \dot{N}_+}{\pi \theta^2 r^2 v_j}, \quad (4)$$

where  $f \equiv \dot{N}_p/\dot{N}_+ = n_p/n_+$  is the ratio of the flux (and so the number density) of protons to that of positrons in the jet. From Figure 6 we know that the opening angle of the jets in 1E 1740.7–2942 is about  $10^\circ$  or less. The speed of the jets can be either close to the speed of light or much smaller; we chose an average value of  $v_j = 0.3c$ . Thus from equation (4), the maximum length a jet can reach,  $r = r_j$ , is

$$r_j = 0.31(1 + 920f)^{1/2} \left(\frac{\dot{N}_+}{10^{42} \text{ s}^{-1}} \frac{v_j}{0.3c}\right)^{1/2} \times \left(\frac{P_I/k}{2.5 \times 10^6 \text{ cm}^{-3} \text{ K}}\right)^{-1/2} \left(\frac{\theta}{10^\circ}\right)^{-1} \text{ pc}. \quad (5)$$

It is clear that, even at the maximum allowable mean positron luminosity, the momentum flux of a pure pair jet ( $f = 0$ ) from 1E 1740.7–2942 is still *not* enough to power the jets to a distance of  $\sim 1$  pc as observed, unless the jets are highly relativistic with a bulk Lorentz factor greater than a few or are extremely well collimated ( $\theta < 2^\circ$ ) or both. Although we cannot rule out either option, the more plausible possibilities that the real jet length is longer than it is projected on the sky and the real pair flux in the jets may be smaller than the maximum value we applied here would suggest that it is more likely that these jets are mixed with at least some protons. Indeed, a mixed jet with merely  $f = 0.02$  or higher in equation

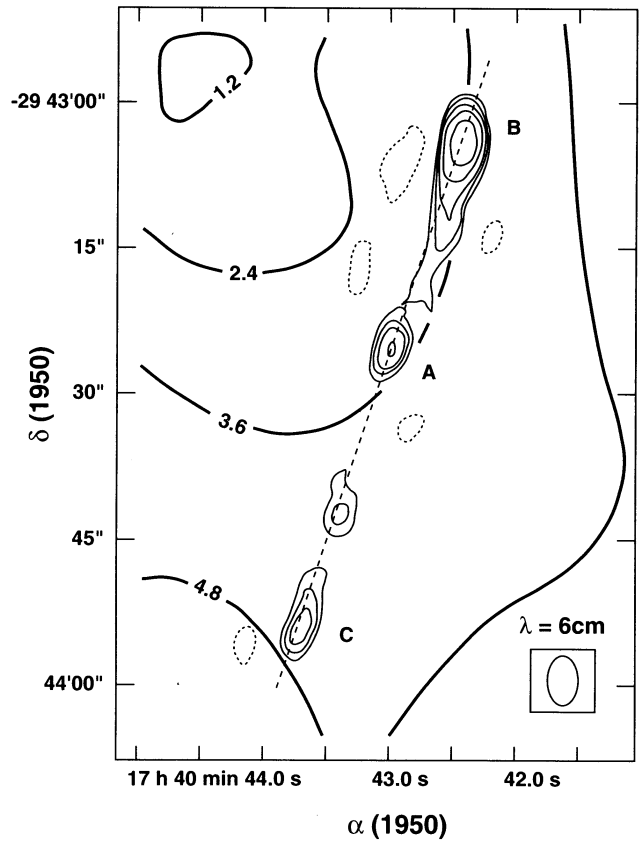


FIG. 6.—The radio jet morphology of 1E 1740.7–2942. The thin solid lines are the 6 cm VLA contour map (Mirabel et al. 1992) overlaid on the  $\text{HCO}^+$  contour (thick solid line) of the molecular cloud along the line of sight of the source (Mirabel et al. 1991). The thin dashed line shows that the sources A, B, and C are well aligned. Slight bending of the jets can be observed. The southern jet AC is longer than the northern jet AB by about 20%.

(5) will suffice to sustain itself to the observed distance. A longer jet would require a larger  $f$ .

#### 4.2. What Is the Proton-Positron Ratio in the Jets?

Before we give this estimate, let us ask another fundamental question: Can the jets of 1E 1740.7–2942 be made of pure proton-electron plasma? There is certainly no problem in this option from the energetics point of view as we have shown above. However, we will argue that a pure  $p-e^-$  jet may not contain enough electrons to produce the observed synchrotron radio flux from the jets. First of all, the maximum proton (also electron) flux injected into the jets can be determined from the maximum mass accretion rate inferred from the observed X-ray luminosity of 1E 1740.7–2942. In its normal state the total X-ray luminosity from ART-P and SIGMA data is  $\sim 3 \times 10^{37}$  ergs  $\text{s}^{-1}$  (Sunyaev et al. 1991b). Since in the ART-P and *Spartan 1's* low-energy X-ray spectra there is no trace of a strong soft component, the total X-ray luminosity from 1E 1740.7–2942 is likely to be no more than  $5 \times 10^{37}$  ergs  $\text{s}^{-1}$  even taking into account the severe absorption in the low-energy band. In the low state, the X-ray flux is reduced by, on average, a factor of 5 (Churazov et al. 1993a). Since the data from the last decade (Fig. 5) indicate that 1E 1740.7–2942 resides in the normal state longer than in the low state, the mean X-ray luminosity is probably  $\sim 3 \times 10^{37}$  ergs  $\text{s}^{-1}$ . This

value corresponds to a mass accretion rate of  $\dot{M} \sim 5 \times 10^{-9}(\eta/0.1)^{-1} M_{\odot} \text{ yr}^{-1}$  assuming a 10% X-ray production efficiency  $\eta$  which is in the range of 5%–30% (e.g., Thorne 1974). This accretion rate is smaller than the Eddington limit of even an  $1 M_{\odot}$  black hole. Since it is generally believed that the mass ejection into the jets (or winds) does not dominate during the sub-Eddington accretion phase (e.g., Shakura & Sunyaev 1973), this mean accretion rate also serves as an upper limit of the mass ejection rate into the jets. The maximum proton (and electron) flux is then  $\dot{N}_{p,e} \leq 2 \times 10^{41} \text{ s}^{-1} (L_x/3 \times 10^{37} \text{ ergs s}^{-1})(\eta/0.1)^{-1}$ . Such an electron flux, multiplied by the travel time along the jet length, gives the total number of injected electrons contained in the jets as  $N_{e^-,inj} \leq 7 \times 10^{49} (L_x/3 \times 10^{37} \text{ ergs s}^{-1})(\eta/0.1)^{-1} (v_j/0.3c)^{-1}$ .

On the other hand, the observed radio synchrotron flux from the jets of a few mJy at 6 cm (Mirabel et al. 1992) implies that (1) the Lorentz factor of the radio emitting particles is on the order of  $\gamma_{\pm} \sim 3 \times 10^3 (B/100 \mu\text{G})^{-1/2}$  for given magnetic field strength  $B$ , and (2) the total number of radio-emitting particles (i.e., having  $\gamma_{\pm} \sim 3 \times 10^3$ ) is  $N_{e^{\pm},\gamma_{\pm}} \sim 10^{46} (B/100 \mu\text{G})^{-1}$  at the GC distance. Since these particles are at the high-energy tail of a presumably power-law spectrum with a nominal spectral index of  $\sim 2$ , the number of nonthermal particles will be  $N_{e^{\pm},NT} \geq 10^6 N_{e^{\pm},\gamma_{\pm}} \sim 10^{52} (B/100 \mu\text{G})^{-2}$  if the low-energy cutoff of the spectrum is less than a few MeV. Furthermore, it is generally believed that the nonthermal particle population is accelerated in the jets rather than in the central source (Begelman et al. 1984) and that the acceleration processes (e.g., the first-order Fermi mechanism via strong shocks in the jets) can *at best* accelerate a few percent of the thermal particles into the nonthermal population (this efficiency is very uncertain, but it is likely to be *much* smaller than we quoted here, see Jones & Ellison 1991). Therefore the total number of thermal and nonthermal leptons in the jets implied by the observed radio flux is likely to have a lower limit of  $N_{e^{\pm},radio} \geq 10^{55} (B/100 \mu\text{G})^{-2}$ .

One immediately notices that the *minimum* number of electrons required by the observed radio flux is about 5 orders of magnitude greater than the *maximum* number of electrons available in the jets if they were made of pure  $p-e^-$  plasma. One could argue that the injected material in the jets can actually be mixed with large amounts of ISM gas when the jets penetrate through the ISM, so the requirement for the injected electron flux could be much lower (Cellotti & Fabian 1993). But even if we drastically increase the electron population by mixing up to 3 orders of magnitude for the case of the most powerful radio galaxies (Cellotti & Fabian 1993), it is still only a few percent of that required by the observed radio flux in 1E 1740.7–2942. There is also morphological evidence which does not favor large mixing in the jets of 1E 1740.7–2942. In Figure 6 we see that the jets not only have prominent radio lobes at the end, but also show continuous structure along their length. Particularly, the flux from the radio spot halfway in the southern jet is no less than 10% of the flux from the lobes. Since one would expect that much more mixing is taking place in the lobes than in the jets, the relatively low spot/lobe contrast may indicate that mixing is not high in the lobes either, i.e., the overall mixing in the jets of 1E 1740.7–2942 is probably much less than the 3 orders of magnitude inferred from the most powerful radio galaxies.

A natural way to resolve this discrepancy is to let the jets in 1E 1740.7–2942 be a mixture of  $p-e^-$  plasma and  $e^+e^-$  pairs. We require that the pairs in the jets dominate in number but

most of the momentum is provided by the protons. The optimal  $p/e^+$  ratio from the maximum proton and positron flux we estimated above is therefore

$$f = 0.2 \left( \frac{L_x}{3 \times 10^{37} \text{ ergs s}^{-1}} \right) \left( \frac{\dot{N}_+}{10^{42} \text{ s}^{-1}} \right)^{-1}, \quad (6)$$

which allows the jet to penetrate into the ISM as far as  $\sim 4.2$  pc. Now the total  $e^{\pm}$ 's in the jets from both pairs and normal plasma is of the order a few times  $10^{51}$ . The radio flux requirement can be fulfilled by allowing the mixing of a factor of  $\leq 10^2$  with the ISM gas and allowing the magnetic fields in the jets and lobes being a few hundred  $\mu\text{G}$ . The latter condition can be satisfied if one argues that the magnetic fields in the jets and lobes are in equipartition with the ISM confinement pressure.

The major conclusions from the analysis of last two sections are that although we cannot exclude the possibility that the jets of 1E 1740.7–2942 are made of either pure pairs or pure normal plasma, it is more natural and fully consistent with all the observational facts that the jets are mixed with both pairs and normal plasma. The optimal proton-positron ratio in the jets is between 2% and 20%.

### 4.3. How Fast Are the Jets Moving?

The velocity of the heads of the jets,  $v_h$ , moving into the ISM is determined by  $\rho_1 v_h^2 = \rho_j (v_j - v_h)^2 \sim \rho_j v_j^2$  (e.g., Begelman, et al. 1984), i.e.,

$$v_h = 0.21(1 + 920f)^{1/2} \left( \frac{\dot{N}_+}{10^{42} \text{ s}^{-1}} \frac{v_j}{0.3c} \right)^{1/2} \times \left( \frac{n_I}{5 \times 10^4 \text{ cm}^{-3}} \right)^{-1/2} \left( \frac{\theta}{10^\circ} \frac{r}{\text{pc}} \right)^{-1} \text{ km s}^{-1}. \quad (7)$$

It decreases linearly with the opening angle and the distance from the core but depends less sensitively on  $\dot{N}_+$ ,  $v_j$ , or  $n_I$ . For  $f = 0.2$  and  $r = 1$  pc, the velocity  $v_h$  is  $\sim 1.6 \text{ km s}^{-1}$ , i.e., the jet is currently propagating into the ISM with a Mach number of merely 2. The time-averaged velocity of the head is roughly  $\bar{v}_h \sim 2v_h \sim 3.2 \text{ km s}^{-1}$ , and so the minimum current age of the jets is

$$\tau_{\text{jet}} \sim 2 \times 10^5 \left( \frac{L_x}{3 \times 10^{37} \text{ ergs s}^{-1}} \frac{v_j}{0.3c} \right)^{-1/2} \times \left( \frac{n_I}{5 \times 10^4 \text{ cm}^{-3}} \right)^{1/2} \left( \frac{\theta}{10^\circ} \frac{r}{\text{pc}} \right) \text{ yr}. \quad (8)$$

We note that our estimates of the jet parameters all depend on the jet speed,  $v_j$ , for which we have adopted a canonical value of  $0.3c$ . A much slower jet is not favored because the positrons in the jet would otherwise annihilate before they reach the end of the jet. The strength of narrow 511 keV line radiation from 1E 1740.7–2942 also depends very much on how successfully the positrons produced near the black hole are transported and deposited into the ISM. Since the density of electrons in the jets is  $n_e = 2(1+f)\dot{N}_+/\pi\theta^2 v_j^2 r^2$ , the probability of a positron annihilating in the jet is

$$P_+(r) = \int \sigma(T_e) n_e c dt = \frac{2(1+f)\sigma(T_e)c\dot{N}_+}{\pi\theta^2 v_j^2} \left( \frac{1}{r_0} - \frac{1}{r} \right), \quad (9)$$

where  $r_0$  is the distance of the base of the jets from the black hole, and  $\sigma(T_e)$  is the annihilation cross section at electron temperature  $T_e$ . From equation (9) it is clear that the survival rate of positrons at large distances is almost completely controlled by their survival rate at the base of the jets. Since the



source accretion rate is sub-Eddington, no significant pair production is expected beyond  $r_0 = 100$  Schwarzschild radii and we expect most of the positrons at this radius to survive to large distances. The annihilation cross section  $\sigma(T_e)$  is nearly a constant at  $T_e \leq 2 \times 10^9$  K and decreases roughly with  $T_e^{-2}$  at higher temperatures (Ramaty & Mezáros 1981). The pair production region near the black hole ( $\leq 10r_s$ ) has a temperature greater than  $10^{12}$  K. At  $r_0 \sim 100r_s$ , the plasma is adiabatically cooled to a few times  $10^{10}$  K. At this temperature the annihilation cross section is about  $0.01\pi r_e^2 = 2.4 \times 10^{-27}$  cm<sup>2</sup>. Thus, the condition  $P_+ < 1$  will be satisfied if

$$v_j > 0.09c \left( \frac{\dot{N}_+}{10^{42} \text{ s}^{-1}} \right)^{1/2} \left( \frac{r_0}{100r_s} \frac{m_{\text{BH}}}{5 M_\odot} \right)^{-1/2} \left( \frac{\theta}{10^\circ} \right)^{-1}, \quad (10)$$

where we have adopted  $f = 0.2$ . We note that a much lower electron temperature at the base of the jets will require a higher jet speed.

There may be a unique and interesting test for the true jet speed. The positrons, which were produced during the strong outburst in 1990 October and are being transported along the jets, will eventually annihilate in the ISM to give a (weak) burst of narrow 511 keV annihilation radiation. While the intensity and duration of the flux increase depend on how many pairs were injected into the jets and on the initial positron energy when they reach the ISM (Ramaty et al. 1992), the time delay of the flux increase depends only on the length of the jets and the jet velocity. If  $v_j$  is close to the speed of light, then we expect the narrow annihilation flux increase to occur sometime after 1994 (minimum time delay assumes the jets are as long as their projection on the sky).

#### 4.4. Constraints on the Core Velocity

Since the 1E 1740.7–2942 jets are not observed to bend and are roughly of equal length, it is probably the case that 1E 1740.7–2942 has been moving very slowly through the ISM during the entire history of the jets; a large transverse (i.e., perpendicular to axis of the jets and to our line of sight) velocity would have caused an apparent bending of the jets and a large parallel velocity would have caused a large difference in the lengths of the two jets.

In Figure 6 we see that the maximum displacement of source A from the jet axis is less than 1/10 of the jet's length, which implies that the transverse velocity of source A in the ISM is  $v_{A,t} < 0.1\bar{v}_h \sim 0.5$  km s<sup>-1</sup>. Along the jets, we notice that the south core-lobe distance (between source A and source C) is about 25% longer than the north core-lobe distance (between source A and source C), which can be explained if source A has been moving to the north with a speed of  $v_{A,p} \sim 0.25\bar{v}_h \sim 1.2$  km s<sup>-1</sup>. However, one may argue that part of the difference in the lengths of the two jets could be caused by the density variation between the north and south directions; the HCO<sup>+</sup> contour map overlaid on the 6 cm radio image indicates that the density near source C is probably lower than that near source B by a factor of 2 which could make the south jet 15% longer than the north one. If this is the case, the parallel velocity of source A is only  $\sim 0.1\bar{v}_h$ . There is no information on the radial velocity of 1E 1740.7–2942. If it is of the same order as the transverse velocity, we may conclude that 1E 1740.7–2942 has been moving in the ISM in the last 200,000 yr probably no faster than  $\sim 2$  km s<sup>-1</sup>. This is much smaller than the velocity dispersion of the molecular cloud ( $> 20$  km s<sup>-1</sup>, Bally & Leventhal 1991; Mirabel et al. 1991).

An alternative is that 1E 1740.7–2942 is not physically associated with the molecular cloud, but instead is residing in an intercloud low-density region. If such a region has a temperature of  $10^5$ – $10^6$  K, its hydrogen number density will be about 10 cm<sup>-3</sup> based on the pressure equilibrium argument. In this case, the jets are moving in the ISM with a much higher speed,  $v_h \sim 140$  km s<sup>-1</sup>, and the source lifetime is much shorter,  $\sim 3400$  yr. The allowed velocity of 1E 1740.7–2942 in the ISM now becomes  $v_A \sim 30$  km s<sup>-1</sup>, which is then consistent with the velocity dispersion of the GC region. The maximum jet length we calculated before, however, will not be affected since it is controlled by the pressure instead of number density.

Since we have little knowledge of the local environment for GRS 1758–258 and there is no dense molecular cloud found along its line of sight, the above analysis on the 1E 1740.7–2942 jets cannot be directly applied to GRS 1758–258. However, the radio maps of GRS 1758–258 (see Rodriguez et al. 1992) reveal some different features of this source: (1) The radio flux from GRS 1758–258 is weaker and the jets are less prominent than in 1E 1740.7–2942. The central source is also less clearly defined due to confused features (source C and D in which C is currently identified as the central source; Rodriguez et al. 1992). The variability of source C during different observations (similar to that of 1E 1740.7–2942) nevertheless supports the identification of source C as the  $\gamma$ -ray source. (2) The double radio lobes are less symmetric in GRS 1758–258 than in 1E 1740.7–2942 and particularly the southern lobe (source A) is twice as far away from source C as the northern lobe (source B). Also there is no direct link (a jet or an elongated feature) between sources B and C. (3) The northern “jet” in GRS 1758–258 is much fatter than the well-collimated jet in 1E 1740.7–2942 though they are about the same length ( $\sim 30''$ ). Its elongated structure does not point toward source C, suggesting bending. These jet characteristics suggest that GRS 1758–258 is probably located in a lower pressure ISM and is moving with greater speed than 1E 1740.7–2942.

#### 5. ACCRETION FROM THE INTERSTELLAR MEDIUM?

Now we consider whether or not the  $\gamma$ -ray sources could be powered by direct accretion from the ISM. This option has the advantages that it does not depend on the uncertain prospects of finding companion stars and that the source accretion rate can be calculated straightforwardly for given ISM conditions. The Bondi-Hoyle accretion luminosity is (Bondi & Hoyle 1944; Bally & Leventhal 1991)

$$\begin{aligned} L_{\text{acc}} &= \eta \pi \mu m_{\text{H}} n_{\text{I}} \frac{G^2 m_{\text{BH}}^2 c^2}{v_{\text{A}}^3} \\ &= 6.6 \times 10^{38} \frac{\eta}{0.1} \frac{n_{\text{I}}}{5 \times 10^4 \text{ cm}^{-3}} \left( \frac{m_{\text{BH}}}{3 M_\odot} \right)^2 \\ &\quad \times \left( \frac{v_{\text{A}}}{2 \text{ km s}^{-1}} \right)^{-3} \text{ ergs s}^{-1}, \quad (11) \end{aligned}$$

which is a factor of 20 higher than the observed luminosity of 1E 1740.7–2942 in the normal state. Since  $v_{\text{A}} \propto v_h \propto n_{\text{I}}^{-1/2}$  (eq. [7]), the accretion luminosity is very sensitive to the environment,  $L_{\text{acc}} \propto n_{\text{I}}^{5/2}$ . Therefore, for  $L_{\text{acc}}$  not to exceed the observed X-ray luminosity ( $\sim 3 \times 10^{37}$  ergs s<sup>-1</sup>),  $n_{\text{I}}$  in the vicinity of 1E 1740.7–2942 is required to be less than

$\sim 1.5 \times 10^4 \text{ cm}^{-3}$  if indeed the source is moving in the ISM at no more than  $2 \text{ km s}^{-1}$ . A black hole mass higher than  $3 M_{\odot}$  would require an even lower ISM density. So even if the source is associated with a dense molecular cloud, it is probably only partially embedded in the outer layer of the cloud, which is consistent with the fact that the total absorption column density toward 1E 1740.7–2942 inferred from *ROSAT* observations is less than half of the column density of the cloud. On the other hand, if 1E 1740.7–2942 were moving in a hot, low-density ( $n_1 \sim 10 \text{ cm}^{-3}$ ) intercloud medium, it would be impossible for the Bondi-Hoyle accretion to power its observed X-ray luminosity, unless the black hole in the system has a mass greater than  $10^4 M_{\odot}$  which is unlikely.

Therefore, the simple accretion power analysis, combined with jet morphology, suggests that 1E 1740.7–2942, if most of its radiation is powered by Bondi-Hoyle accretion, is located in an ISM region of density no more than  $10^4 \text{ cm}^{-3}$  which is, at best, in the outskirts of the dense molecular cloud along its line of sight. GRS 1748–258 could be in an ISM of similar density but lower pressure since it is several degrees away from the highly pressurized central GC region.

### 5.1. Moving through Dense Clumps in a Molecular Cloud?

In addition to placing severe constraints on where in the ISM 1E 1740.7–2942 is located, the radio jet geometry also sheds light on how the observed long-term variability is produced. Since the accretion luminosity depends on the ISM density so sensitively, an order of magnitude variation in the X-ray flux requires only a factor of 2.5 contrast in ISM density. Our question is then, is it possible that the long-term variation of the X-ray luminosity from 1E 1740.7–2942 and GRS 1758–258 are caused by motion through the density fluctuations in the ISM (or a molecular cloud)?

Studies of the ISM in the solar neighborhood show that most giant molecular clouds are actually made of numerous dense clumps which make up 60%–90% of the mass and have a volume filling factor on the order 2%–3% and a density contrast of  $\geq 10$  with the interclump medium inside the cloud (e.g., Blitz 1993). The relative velocity between the clumps is small, typically a few  $\text{km s}^{-1}$  or less. The mass distribution of the clumps follows a power law of slope approximately  $-1.6$  for over three orders of magnitude in mass from about  $1 M_{\odot}$  to  $3000 M_{\odot}$ . Most of the clumps are held together not by their self-gravitation but by the pressure in the interclump medium and have similar densities of  $\sim 10^3 \text{ cm}^{-3}$ ; the sizes of the clumps range from 0.2 pc to 3 pc.

Such a universal clumpy structure of giant molecular clouds could support the ISM accretion hypothesis, but we find that the numbers do not work out. Although there may be some differences between the cloud structure in the local ISM and the GC region, the local information, nevertheless, can serve as a guide to what we may expect from a GC cloud (if we are allowed to scale the local cloud pressure and density up to the GC values). The observed small interclump velocity is comparable to the source velocity we inferred for 1E 1740.7–2942 from the radio jet kinematics, so there is no problem in terms of adequate accretion luminosity. The small density contrast required by the observed variation amplitude implies that the source may be only passing through the *edge* of the clumps where the density is less.

To make this scenario work, however, requires very small clump sizes and a small ratio of the of the interclump distances to the clump sizes. The observed long-term variation timescale

is from a few months to 1 yr. For a relative velocity of a few  $\text{km s}^{-1}$ , this timescale corresponds to a clump size of at most  $10^{-5}$  pc, which is much smaller than the smallest clumps ever detected. Even if we scale the clump density to  $10^5 \text{ cm}^{-3}$  as observed in the GC region, a  $1 M_{\odot}$  clump size is still more than 3 orders of magnitude greater than is required. On the other hand, the X-ray light curve of 1E 1740.7–2942 indicates that the source stays in the normal state longer than in the low state, suggesting that the dense region is greater or at least not smaller in size than the less dense region. This would directly contradict the fact that the dense clumps have a small volume filling factor. Therefore, the only possible scenario under these conditions is that the observed accretion rate variations are caused by density fluctuations (by a factor of 2) of length scale of  $\sim 1 \text{ AU}$  near the surface of a clump; to observe such fine structures even in the local molecular clouds (say, 100 pc away) requires a spatial resolution of 0.007 which is beyond the best current millimeter telescope resolutions.

The biggest difficulty in adopting this scenario lies in the fact that GRS 1758–258 has not yet been found to be aligned with any dense molecular cloud. The relatively low X-ray absorption column depth observed from GRS 1758–258 (Skinner 1991) would argue against a physical association even if one finds an apparent alignment. Thus, it is unlikely that the long-term variabilities seen in GRS 1758–258 are caused by passage through density fluctuations in a giant molecular cloud. However, a common origin is strongly suggested by the striking similarities in the variation amplitudes and timescales between the two sources.

### 5.2. Self-Regulated Accretion Flow?

In the Bondi-Hoyle accretion hypothesis, a common origin of the long-term variability for both 1E 1740.7–2942 and GRS 1758–258 may be possible if the accretion flow can be self-regulated by the emerging X-ray flux. In the case of spherical accretion, it has long been pointed out (Buff & McCray 1974; Ostriker et al. 1976; Cowei, Ostriker, & Stark 1978) that X-rays produced close to the central object can ionize and heat the infalling gas so that a thermal pressure gradient builds up in the flow. For certain values of the X-ray continuum luminosity and the X-ray production efficiency, the preheating becomes disruptive via a thermal instability (Krolik & London 1983) and a steady state accretion flow can no longer exist (e.g., Ostriker et al. 1976). A possible consequence is that, if substantial preheating occurs outside the sonic point (the radius at which the accretion flow smoothly becomes transonic), the accretion rate and then the emerging X-ray flux will display a (quasi-)cyclic behavior (Cowe et al. 1978): the strong preheating causes the sonic point to shrink which in turn reduces the accretion rate dramatically and so the X-ray luminosity starts to fall; with less X-rays and so less preheating, the gas cools and the sonic point moves outward which then causes the accretion rate and the X-ray flux to increase again. If, on the other hand, the preheating occurs largely inside the sonic point, the average accretion rate will roughly be a constant but the X-ray luminosity displays (ir)regular flares (Cowe et al. 1978; Grindlay 1978).

Despite the attractiveness of the self-regulated accretion mechanism to produce large-amplitude X-ray variations on long-term timescales, there are several questions to be answered. First, most of the previous work was dealing with a spherically symmetric accretion flow. In the case of 1E 1740.7–2942 and GRS 1758–258, the sources are moving

in the ISM supersonically (with a Mach number of a few). Whether and how the self-regulation mechanism will work in such cases is not clear. Second, for black hole candidates like 1E 1740.7–2942 and GRS 1758–258, the emerging X-ray spectra are much harder ( $> 10$  keV) than that of neutron stars ( $< 10$  keV) considered by previous authors. The hard X-rays ionize the accretion gas less efficiently and produce free electrons at much higher energies. So the thermalization timescale (i.e., the heating timescale) of the high-energy electrons with ions is much longer than that of low-energy electrons. When this timescale becomes longer than the flow timescale, significant heating of the accretion gas will not occur. And third, a more serious and generic problem of the self-regulation mechanism is that, once the accretion flow becomes unstable due to strong preheating, it is not at all certain that the flow will follow the (quasi-) cyclic prescription we have described above. The spherical symmetry may break up and the accretion flow may become lumpy to ensure efficient cooling so that it can still fall in without being significantly slowed down. It is also possible that the interaction between the accretion flow and the emerging X-ray flux can be tuned so that the X-ray emission will be marginally balanced by a steady, self-adjusted accretion rate (Cowie et al. 1978).

## 6. ACCRETION FROM A COMPANION STAR?

Placing 1E 1740.7–2942 and GRS 1758–258 in low-mass binary systems will ensure that a stable accretion disk can form so that energy and/or mass expelled along its rotation axis will naturally give the well-collimated radio jets as observed. However, it is not clear in this scheme that one can produce the observed long-term hard X-ray variabilities. The variabilities cannot be due to the binary orbital modulation, because the orbital period is probably  $\leq 20$  hr (§ 2.3) and the observed variabilities are not periodic and are of much longer timescales. There has been no previous work done on how to produce long-term, large-amplitude nonperiodic variabilities in low-mass X-ray binaries. In this section, we discuss two options in analogy to the similar time signatures observed in cataclysmic variables (CVs) in which the primary accreting object is a white dwarf.

### 6.1. Solar Cycle Activities?

Late-type stars have long-term (quasi-)cyclic chromospheric activities like the Sun. Due to the varying number of magnetic flux tubes (and so the magnetic pressure support) over the activity cycle, the stellar radius could vary by as much as  $\Delta R/R \sim 5 \times 10^{-4}$  or more (e.g., Thomas 1979). For such a star being the Roche lobe filling secondary in a close binary, the mass overflow rate through the Lagrangian point may be modulated by the radius variation. Thus it has been suggested (Warner 1988) that this mechanism is responsible for the observed (quasi-)periodic, long-term variations in mean brightness of some CVs (e.g., Bianchini 1992).

The mass transfer rate in a Roche lobe filling binary is  $\dot{M} \propto e^{\Delta R/H}$  (Osaki 1985), where  $H$  is the pressure scale height of the upper atmosphere of the secondary and  $H/R \sim 3.2 \times 10^{-4}$  for a low-mass main-sequence star. Therefore, we have (Warner 1988)

$$\dot{M} = \dot{M}_0 e^{3100\Delta R/R}, \quad (12)$$

where  $\dot{M}_0$  is the normal mass transfer rate. If the radius variation of the secondary is greater than  $5 \times 10^{-4}$ , it could cause

the mass transfer rate to change by as much as a factor of 5 which would suffice to explain the observed variabilities in 1E 1740.7–2942 and GRS 1758–258. However, problems with this scenario are that (1) the solar-cycle activities are (quasi-)periodic while the observed variations in 1E 1740.7–2942 and GRS 1758–258 are probably not; (2) even if they are shown by future observations to be quasi-periodic, it is hard to believe that the activity periods in 1E 1740.7–2942 and GRS 1758–258 would be so similar since such periods in CVs have a large spread between less than 1 yr and more than 20 yr (Bianchini 1992); and (3) this scenario would predict that the systems are mostly residing in the low state (when the magnetic activities are low) and become brighter only within the limited time period when the secondary star becomes active. This is not what we have seen in 1E 1740.7–2942 and GRS 1758–258.

### 6.2. Structural Adjustment or Stellar Spots of the Companion?

Another possibility for producing long-term variabilities in low-mass X-ray binaries in analogy to that in CVs is based on the fact that the optical brightness of a special subclass of CVs, called VY Scl (or TT Ari) stars, show long-term irregular variabilities (Hudec, Huth, & Fuhrmann 1984) with timescales and amplitudes similar to that observed in 1E 1740.7–2942 and GRS 1758–258. These stars are bright for most of the time and only occasionally become dimmer by a few magnitudes for an extended period of time ranging from a few months to a few years. All VY Scl stars have a binary period of  $\sim 3$  hr which is at the upper boundary of the so-called CV period gap (a gap in the CV period distribution between 2 and 3 hr; e.g., Peterson 1984). The formation of the period gap is thought to be due to the evolution of the low-mass ( $\sim 0.3 M_\odot$ ) secondary star (Peterson 1984). At a certain stage of the evolution the star undergoes internal structural adjustment and its radius shrinks. It therefore does not fill its Roche lobe anymore and the mass transfer (and accretion activity) stops. The system then gradually loses its orbital angular momentum due to gravitational radiation. The Roche lobe radius slowly decreases until it touches the surface of the secondary star again (orbital period about 2 hr) and accretion resumes.

For VY Scl stars, it has been argued that the long-term, irregular variations reflect the abortive attempt of a star near the period gap to cease its mass transfer rate before it eventually enters the period gap (e.g., Robinson et al. 1981). So the characteristic of the variations would be that the systems stay in the high rate most of the time and only occasionally plunge into the low state. However, recent calculations (Ritter 1988) show that the timescale for such structure adjustment is much longer ( $\geq 10^4$  yr) than that observed in VY Scl stars. A new scenario has been proposed recently (Livio & Pringle 1994) in which the dips in the mass transfer rate seen in VY Scl stars occur when a starspot (similar to a sunspot) covers the  $L_1$  point. The required growing size of the starspots as the system approaches the period gap is thought to be due to rotationally enhanced surface magnetic field strength ( $\geq 10^3$  G) on the secondary whose spin period is tidally locked to the binary period. We do not yet know if this is the correct explanation for the VY Scl stars or if it is at all reasonable to apply it to black hole binaries. We raise this option because the scenario depends *only* on the properties of the low-mass secondary star. Therefore, if this mechanism is viable for the VY Scl type of CVs, it will not discriminate against a black hole or neutron star system as long as the latter has a similar secondary com-

panion. A direct consequence of this proposition is that the secondary stars in our  $\gamma$ -ray sources would also be much less than  $1 M_{\odot}$  so it would be impossible to detect them at the GC distance (see Fig. 2).

#### 7. BONDI-HOYLE ACCRETION ONTO A BINARY

As discussed above, it is difficult to produce the observed long-term hard X-ray variabilities in 1E 1740.7–2942 and GRS 1758–258 in a low-mass binary system. On the other hand, it is difficult to create and maintain a *stable* accretion disk (which is essential for the collimation of the radio jets) when a black hole travels and accretes from randomly oriented density fluctuations in the ISM. A possible scenario to overcome these difficulties is to combine the virtues of the two models and have binary systems plus accretion from the ISM. It is conceivable that a black hole binary system moving through the high-density environment of the GC will accrete gas anyway, in addition to the binary accretion. When the sources are moving slowly in the ISM, the total accretion rate from Bondi-Hoyle accretion could be greater than that from the binary accretion. It is possible in this case that the interaction between the X-rays and the surrounding medium will self-regulate the accretion rate which will give rise to the observed long-term hard X-ray variabilities. On the other hand, the orbital plane of the binary will ensure the formation of a stable accretion disk. The gas accreted from the ISM will also fall onto this disk before it is eventually accreted onto the black hole. This scenario thus allows for: (1) a low-mass companion consistent with current IR upper limits; (2) an accretion disk to form a stable jet; and (3) plenty of accretion power from the ISM. It is not easy to prove but the key indicators would be a companion star detected in the IR at  $K \approx 20$  and evidence of a (partially) ionized accretion region in radio, millimeter, or IR.

#### 8. CONCLUSIONS

We have shown that a more detailed analysis of the X-ray absorption column density toward 1E 1740.7–2942 gives a more restricted range of  $(0.5\text{--}1.1) \times 10^{23} \text{ cm}^{-2}$  and indicates that the source is at most only partially embedded in the molecular cloud projected in its direction. We found that the current optical and near-IR upper limits severely constrain the properties of the potential companion stars in 1E 1740.7–2942 and GRS 1758–258. Massive companions can be largely ruled out. These systems must be close low-mass

binaries if most of their X-ray emission is from Roche lobe accretion. For GRS 1758–258,  $K$ -band IR imaging to as deep as 19th mag could detect a sub-solar-mass main-sequence companion, while for 1E 1740.7–2942 it will be much more difficult to find a low-mass companion if the total column density toward the source is  $\sim 10^{23} \text{ cm}^{-2}$ . We see from Figure 2 that, for  $A_V = 25$ , one can detect a  $2 M_{\odot}$  star at  $K = 19$  or an  $1 M_{\odot}$  star at  $K = 21$ . These limiting magnitudes are achievable using the current best large telescopes, so the optical/IR counterpart search should continue.

The analysis of the energetics, morphology, and the radio flux of the radio jets in 1E 1740.7–2942 suggests that they are probably made of both  $e^+e^-$  pairs and (a few to a few tens of percent) normal plasma and that the velocity at which the source is moving in the ISM is probably small ( $< 10 \text{ km s}^{-1}$ ). While the age of the sources may be on the order of  $10^5 \text{ yr}$ , it is hard to imagine that a stable rotation axis of the accretion disk can be maintained if 1E 1740.7–2942 is accreting directly from the nearby high-density molecular cloud.

Combining the radio jet analysis and the observed long-term hard X-ray variabilities, we have tried to identify plausible mechanisms to produce these observational features in both the Bondi-Hoyle accretion and the binary accretion schemes. Both schemes have their merits. While the accretion flow from the ISM may be more easily regulated by its interaction with the emerging X-ray emissions, the accretion disks in binaries can readily provide a stable rotation axis to accommodate the well-collimated radio jets. We thus speculate that in 1E 1740.7–2942 and GRS 1758–258 a combination of both mechanisms is active, i.e., they are binary systems with a stellar mass ( $3\text{--}10 M_{\odot}$ ) black hole and a low-mass ( $\sim 1 M_{\odot}$ ) companion, accreting mainly from the ISM. Deep near-IR imaging to search for the potential companion stars is still a top priority in this endeavor. Theoretical study of the instability and time-dependent behavior of Bondi-Hoyle accretion flow onto black holes and of the low-mass star's evolution is strongly encouraged.

We thank Eugene Churazov for providing the long-term SIGMA data and for pointing out a mistake in the original manuscript. Helpful conversations with and comments from Felix Mirabel, Philippe Durouchoux, Gerry Skinner, Jim Pringle, Marat Gilfanov, Sergei Grebenev, Julian Krolik, Mario Livio, and Andy Fabian are gratefully acknowledged.

#### REFERENCES

- Bally, J., & Leventhal, M. 1991, *Nature*, 353, 234  
 Bally, J., Stark, A. A., Wilson, R. W., & Henkel, C. 1988, *ApJ*, 324, 223  
 Bazzano, A., La Padula, C., Ubertini, P., & Sood, R. K. 1992, *ApJ*, 385, L17  
 Begelman, M. C., Blandford, R. D., & Rees, M. J. 1984, *Rev. Mod. Phys.*, 56, 255  
 Bianchini, A. 1992, in *Vina Del Mar Workshop on Cataclysmic Variable Stars*, ed. N. Vogt (ASP Conf. Ser. 30), 284  
 Blitz, L. 1993, in *Protostars & Planets III*, ed. E. H. Levy & J. I. Lunine, in press  
 Blitz, L., Binney, J., Lo, K. Y., Bally, J., & Ho, P. T. P. 1993, *Nature*, 361, 417  
 Bondi, H., & Hoyle, F. 1944, *MNRAS*, 104, 21  
 Bouchet, L., et al. 1991, *ApJ*, 383, L45  
 Buff, J., & McCray, R. 1974, *ApJ*, 189, 147  
 Burgarella, D., Livio, M., & O'Dea, C. ed. 1993, *Astrophysical Jets* (Cambridge: Cambridge Univ. Press)  
 Cassinelli, J. P. 1979, *ARA&A*, 17, 275  
 Cellotti, A., & Fabian, A. C. 1993, *MNRAS*, 264, 228  
 Churazov, E., et al. 1993a, *ApJ*, 407, 752  
 ———. 1993b, in the *Proc. INTEGRAL Symp.* (1993 Feb., Les Diablerets), in press  
 Cook, W. R., Grunsfeld, J. M., Heindl, W. A., Palmer, D. M., Prince, T. A., Schindler, S. M., & Stone, E. C. 1991, *ApJ*, 372, L75  
 Cordier, B., Paul, J., & Hameury, J. M. 1993a, in *Proc. INTEGRAL Symp.* (1993 Feb., Les Diablerets), in press  
 Cordier, B., et al. 1993b, *A&A*, 97, 177  
 Covault, C. E., Manandhar, R. P., & Grindlay, J. E. 1991, *Proc. 22nd Internat. Cosmic-Ray Conf.* (Dublin), 1, 21  
 Cowei, L. L., Ostriker, J. P., & Stark, A. A. 1978, *ApJ*, 226, 1041  
 Davidson, K., & Ostriker, J. P. 1973, *ApJ*, 179, 585  
 Djorgovski, S., Thompson, D., Mazzarella, J., & Klemola, A. 1992, *IAU Circ.*, No. 5596  
 Gehrels, N., & Tueller, J. 1993, *ApJ*, 407, 597  
 Gilfanov, M., et al. 1993, *ApJ*, 418, 844  
 Grindlay, J. E. 1978, *ApJ*, 221, 234  
 Heindl, W. A., et al. 1994, in preparation  
 Hertz, P., & Grindlay, J. E. 1984, *ApJ*, 278, 137  
 Hudec, R., Huth, H., & Fuhrmann, B. 1984, *Observatory*, 104, 1  
 Johnson, H. L. 1966, *ARA&A*, 4, 193  
 Jones, F. C., & Ellison, D. C. 1991, *Space Sci. Rev.*, 58, 259  
 Kawai, N., Fenimore, E. E., Middleditch, J., Cruddace, R. G., Fritz, G. G., Snyder, W. A., & Ulmer, M. P. 1988, *ApJ*, 330, 130  
 Krolik, J. H., & London, R. A. 1983, *ApJ*, 267, 18  
 Leahy, D. A., Langill, P., & Kwok, S. 1992, *A&A*, 259, 209  
 Lebofsky, M. J., Rieke, G. H., & Tokunaga, A. T. 1982, *ApJ*, 263, 736

- Liang, E. P., & Nolan, P. L. 1984, *Space Sci. Rev.*, 38, 353
- Lingenfelter, R. E., & Ramaty, R. 1989, in *The Center of the Galaxy*, ed. M. Morris (Dordrecht: Kluwer), 587
- Livio, M. 1994, in *22nd Saas-Fee Advanced Courses: Interacting Binaries*, ed. H. Nussbaumer & A. Orr (New York: Springer-Verlag), 135
- Livio, M., & Pringle, J. E. 1994, *ApJ*, in press
- Mandrou, P., et al. 1993, in *Proc. INTEGRAL Symp. (1993 Feb., Les Diablerets)*, in press
- Mereghetti, S., Caraveo, P., Bignami, G. F., & Belloni, T. 1992, *A&A*, 259, 205
- Mirabel, I. F. 1992, *Messenger*, 73, 51
- Mirabel, I. F., & Duc, P. A. 1992, *IAU Circ.*, No. 5655
- Mirabel, I. F., Morris, M., Wink, J., Paul, J., & Cordier, B. 1991, *A&A*, 251, L43
- Mirabel, I. F., Rodriguez, L. F., Cordier, B., Paul, J., & Lebrun, F. 1992, *Nature*, 358, 215
- . 1993, *A&AS*, 97, 193
- Osaki, Y. 1985, *A&A*, 144, 369
- Ostriker, J. P., McCray, R., Weaver, R., & Yahil, A. 1976, *ApJ*, 208, L61
- Peterson, J. 1984, *ApJS*, 54, 443
- Prince, T., & Skinner, G. 1991, *IAU Circ. No. 5252*
- Purcell, W., et al. 1992, in *Compton Gamma-Ray Observatory*, ed. M. Friedlander, N. Gehrels & D. J. Macomb (New York: AIP), 107
- Ramaty, R., Leventhal, M., Chan, K. W., & Lingenfelter, R. E. 1992, *ApJ*, 392, L63
- Ramaty, R., & Lingenfelter, R. E. 1991, in *Gamma-Ray Line Astrophysics*, ed. Ph. Durouchoux & N. Prantzos (New York: AIP), 67
- Ramaty, R., & Mészáros, P. 1981, *ApJ*, 250, 384
- Rieke, G. H., & Lebofsky, M. J. 1985, *ApJ*, 288, 618
- Ritter, H. 1988, *A&A*, 202, 93
- Robinson, E. L., Barker, E. S., Cochran, A. L., Cochran, W. D., & Nather, R. E. 1981, *ApJ*, 251, 611
- Rodriguez, L. F., Mirabel, I. F., & Marti, J. 1992, *ApJ*, 401, L15
- Roques, J.-P. 1993, in *Second Compton Symposium (College Park, 1993 Sep.)*, in press
- Savage, B. D., & Mathis, J. S. 1979, *ARA&A*, 17, 73
- Shakura, N. I., & Sunyaev, R. 1973, *A&A*, 24, 337
- Shu, F., Adams, F., & Lizano, S. 1987, *ARA&A*, 25, 23
- Skinner, G. K. 1991, in *Gamma-Ray Line Astrophysics*, ed. Ph. Durouchoux & N. Prantzos (New York: AIP), 358
- Skinner, G. K., et al. 1991, *A&A*, 252, 172
- . 1987, *Nature*, 330, 544
- Sunyaev, R., et al. 1991a, in *Gamma-Ray Line Astrophysics*, ed. Ph. Durouchoux & N. Prantzos (New York: AIP), 29
- . 1991b, *Sov. Astron. Lett.*, 17, 50
- . 1991c, *ApJ*, 383, L49
- Thomas, J. H. 1979, *Nature*, 280, 662
- Thorne, K. S. 1974, *ApJ*, 191, 507
- Warner, B. 1988, *Nature*, 336, 129